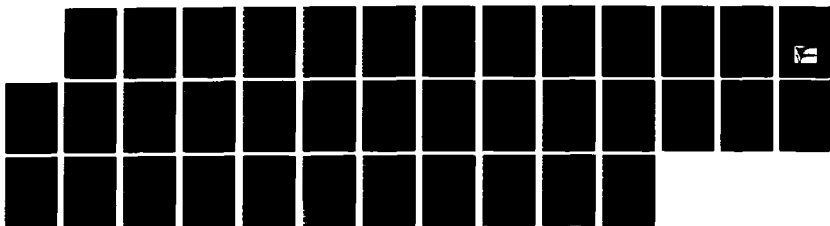


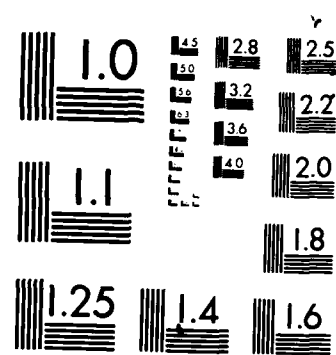
AD-A172 988 STUDY OF SUBMICRON PARTICLE SIZE DISTRIBUTIONS BY LASER 1/1
DOPPLER MEASUREME (U) AERODYNE RESEARCH INC BILLERICA
MA K E MCCURDY ET AL 18 FEB 86 ARI-RR-584

UNCLASSIFIED AFOSR-TR-86-8873 F49620-83-C-0154

F/G 21/2

ML





MICROCOPY RESOLUTION TEST CHART
NATIONAL BUREAU OF STANDARDS 1963-A

FILE COPY

AD-A172 980

(2)

AERODYNE RESEARCH, Inc.
AERODYNE RESEARCH, Inc.

SEARCH, Inc.
SEARCH, Inc.
SEARCH, Inc.
SEARCH, Inc.
SEARCH, Inc.
SEARCH, Inc.
SEARCH, Inc.
SEARCH, Inc.
SEARCH, Inc.

AERODYNE RESEARCH, Inc.
AERODYNE RESEARCH, Inc.
AERODYNE RESEARCH, Inc.
AERODYNE RESEARCH, Inc.
AERODYNE RESEARCH, Inc.
AERODYNE RESEARCH, Inc.
AERODYNE RESEARCH, Inc.
AERODYNE RESEARCH, Inc.
AERODYNE RESEARCH, Inc.
AERODYNE RESEARCH, Inc.
AERODYNE RESEARCH, Inc.
AERODYNE RESEARCH, Inc.
AERODYNE RESEARCH, Inc.
AERODYNE RESEARCH, Inc.
AERODYNE RESEARCH, Inc.
AERODYNE RESEARCH, Inc.
AERODYNE RESEARCH, Inc.
AERODYNE RESEARCH, Inc.
AERODYNE RESEARCH, Inc.
AERODYNE RESEARCH, Inc.

DISTRIBUTION STATEMENT A

Approved for public release
Distribution Unlimited

DTIC
ELECTE
OCT 9 1986
S D
B 46

AERODYNE
RESEARCH, Inc.

 45 Manning Road
The Research Center at Manning Park
Billerica, Massachusetts 01821

AFOSR-TR-86-0873

ARI-RR-504

STUDY OF SUBMICRON PARTICLE SIZE
DISTRIBUTIONS BY LASER DOPPLER
MEASUREMENT OF BROWNIAN MOTION

Annual Technical Report

Prepared by

Keith E. McCurdy, Alan C. Stanton, and Wai K. Cheng
Aerodyne Research, Inc.
45 Manning Road
Billerica, MA 01821

Prepared for

Air Force Office of Scientific Research
Building 410
Bolling AFB, DC 20332

Contract No. F49620-83-C-0154

DTIC

OCT 9 1986

February 1986

Approved for public release;
distribution unlimited.

Approved for public release; distribution unlimited.
This report contains neither recommendations nor conclusions of the Air Force Office of Scientific Research. It has been reviewed by the AFOSR and approved for public release. Distribution outside AFOSR is controlled by AFOSR.
111-86-0873
This report contains neither recommendations nor conclusions of the Air Force Office of Scientific Research. It has been reviewed by the AFOSR and approved for public release. Distribution outside AFOSR is controlled by AFOSR.
111-86-0873

86 10 3 006

UNCLASSIFIED

SECURITY CLASSIFICATION OF THIS PAGE

10-4172950

REPORT DOCUMENTATION PAGE

1a. REPORT SECURITY CLASSIFICATION UNCLASSIFIED		1b. RESTRICTIVE MARKINGS NONE										
2a. SECURITY CLASSIFICATION AUTHORITY		3. DISTRIBUTION/AVAILABILITY OF REPORT UNLIMITED										
2b. DECLASSIFICATION/DOWNGRADING SCHEDULE												
4. PERFORMING ORGANIZATION REPORT NUMBER(S) ARI-RR-504		5. MONITORING ORGANIZATION REPORT NUMBER(S) AFOSR-TR. 86-0873										
6a. NAME OF PERFORMING ORGANIZATION Aerodyne Research, Inc.	6b. OFFICE SYMBOL (If applicable)	7a. NAME OF MONITORING ORGANIZATION Air Force Office of Scientific Research										
7c. ADDRESS (City, State, and ZIP Code) 45 Manning Road Billerica, MA 01821		7b. ADDRESS (City, State, and ZIP Code) Bolling AFB, Washington, D.C. 20332-6448										
8a. NAME OF FUNDING/SPONSORING ORGANIZATION Air Force Office of Scien. Res.	8b. OFFICE SYMBOL (If applicable) AFOSR/NA	9. PROCUREMENT INSTRUMENT IDENTIFICATION NUMBER F49620-83-C-0154										
10c. ADDRESS (City, State, and ZIP Code) Bolling AFB, Washington, D.C. 20332-6448		10. SOURCE OF FUNDING NUMBERS PROGRAM ELEMENT NO. 61102F PROJECT NO. 2308 TASK NO. A2 WORK UNIT ACCESSION NO.										
11. TITLE (Include Security Classification) (U) "Study of Submicron Particle Size Distributions by Laser Doppler Measurement of Brownian Motion"												
12. PERSONAL AUTHOR(S) Keith E. McCurdy, Alan C. Stanton, and Wai K. Cheng												
13a. TYPE OF REPORT Annual	13b. TIME COVERED FROM 9/1/84 TO 9/30/85	14. DATE OF REPORT (Year, Month, Day) 1986 February 10	15. PAGE COUNT 32									
16. SUPPLEMENTARY NOTATION												
17. COSATI CODES <table border="1"><tr><th>FIELD</th><th>GROUP</th><th>SUB-GROUP</th></tr><tr><td>21</td><td>02</td><td></td></tr><tr><td>21</td><td>05</td><td></td></tr></table>		FIELD	GROUP	SUB-GROUP	21	02		21	05		18. SUBJECT TERMS (Continue on reverse if necessary and identify by block number) Submicron Particles, Brownian Motion, Size Distributions	
FIELD	GROUP	SUB-GROUP										
21	02											
21	05											
19. ABSTRACT (Continue on reverse if necessary and identify by block number) Few nonintrusive techniques are available for particle measurement in the submicron size range (< 0.1 μ m diameter), yet measurement of these particles is basic to an understanding of important processes in combustion, such as soot formation and oxidation. The objective of the present research is the development and application of a technique for measurement of individual submicron particles in a gas stream. The approach is to measure the inertial relaxation time of individual particles of Brownian motion, by statistical analysis of the time-resolved (100 MHz) heterodyne signal obtained in an interferometer system resembling a more conventional laser Doppler velocimeter.												
20. DISTRIBUTION/AVAILABILITY OF ABSTRACT <input checked="" type="checkbox"/> UNCLASSIFIED/UNLIMITED <input type="checkbox"/> SAME AS RPT. <input type="checkbox"/> DTIC USERS		21. ABSTRACT SECURITY CLASSIFICATION UNCLASSIFIED										
22a. NAME OF RESPONSIBLE INDIVIDUAL Dr. Julian Tishkoff		22b. TELEPHONE (Include Area Code) (202) 767-4935	22c. OFFICE SYMBOL AFOSR/NA									

19. Abstract (continued)

the statistical behavior of the signal from such a measurement signal has been developed. From the theory, the probability distribution for the time intervals between the zeros of the Brownian motion velocity may be obtained.

Continuing research on this program will focus on measurements of particles of known size suspended in liquids in order to maximize the signal to noise of the optical measuring system, to refine the data acquisition methods, and to verify the theoretical understanding of the acquired signal. Following the demonstration of the experimental approach, the technique will be applied to measurements of submicron particles suspended in gas flows.

1. RESEARCH OBJECTIVES (STATEMENT OF WORK)

The research objectives for this program are outlined in the Statement of Work, which includes the following tasks:

Task I - The contractor shall construct a laser diagnostic apparatus to be used for submicron particle size analysis by measurement of Brownian motion. The development of this apparatus shall include:

- a) Construction and assembly of relevant optical components;
- b) Adaptation of suitable data acquisition and recording apparatus; and
- c) Development of appropriate software for analysis of signals obtained from the Brownian motion instrument.

Task II - Using the optical apparatus and data recording and analysis tools developed in Task I, the contractor shall investigate the development of optical heterodyne techniques to be used in measurement of the Brownian motion of individual particles. Specifically, techniques are required which permit measurements of motion where the particle velocity changes in distances shorter than one light wavelength.

Task III - Using the instrumentation and techniques developed in Tasks I and II, the contractor shall analyze the statistics of particle motion in the gas to investigate the particle mass, friction coefficient, and equilibrium temperature. These studies shall be conducted under carefully controlled flow conditions, initially using standard size particles. Subsequent development of the technique may utilize a well-characterized flat-flame burner.

Task IV - The contractor shall investigate the measurement of the refractive index of particles in the Rayleigh scattering regime by analysis of the scattered light intensity and particle mass (size) obtained using the Brownian motion sensor.

Task V - By application of the Brownian motion sensor in a flat-flame burner, the contractor shall assess the application of this technique for in-situ sizing of submicron particles in combustion streams.

A-1000-1000

1000-1000

1000-1000

1000-1000

1000-1000

1000-1000

1000-1000

1000-1000

1000-1000

1000-1000

1000-1000

1000-1000

1000-1000

1000-1000

1000-1000

1000-1000

1000-1000

1000-1000

1000-1000

1000-1000

1000-1000

1000-1000

1000-1000

1000-1000

1000-1000

1000-1000

1000-1000

1000-1000

1000-1000

1000-1000

1000-1000

1000-1000

1000-1000

1000-1000

1000-1000

1000-1000

1000-1000

1000-1000

1000-1000

1000-1000

1000-1000

1000-1000

1000-1000

1000-1000

1000-1000

1000-1000

1000-1000

1000-1000

1000-1000

1000-1000

1000-1000

1000-1000

1000-1000

1000-1000

1000-1000

1000-1000

1000-1000

1000-1000

1000-1000

1000-1000

1000-1000

1000-1000

1000-1000

1000-1000

1000-1000

1000-1000

1000-1000

1000-1000

1000-1000

1000-1000

1000-1000

1000-1000

1000-1000

1000-1000

1000-1000

1000-1000

1000-1000

1000-1000

1000-1000

1000-1000

1000-1000

1000-1000

1000-1000

1000-1000

1000-1000

1000-1000

1000-1000

1000-1000

1000-1000

1000-1000

1000-1000

1000-1000

1000-1000

1000-1000

1000-1000

1000-1000

1000-1000

1000-1000

1000-1000

1000-1000

1000-1000

1000-1000

1000-1000

1000-1000

1000-1000

1000-1000

1000-1000

1000-1000

1000-1000

1000-1000

1000-1000

1000-1000

1000-1000

1000-1000

1000-1000

1000-1000

1000-1000

1000-1000

1000-1000

1000-1000

1000-1000

1000-1000

1000-1000

1000-1000

1000-1000

1000-1000

1000-1000

1000-1000

1000-1000

1000-1000

1000-1000

1000-1000

1000-1000

1000-1000

1000-1000

1000-1000

1000-1000

1000-1000

1000-1000

1000-1000

1000-1000

1000-1000

1000-1000

1000-1000

1000-1000

1000-1000

1000-1000

1000-1000

1000-1000

1000-1000

1000-1000

1000-1000

1000-1000

1000-1000

1000-1000

1000-1000

1000-1000

1000-1000

1000-1000

1000-1000

1000-1000

1000-1000

1000-1000

1000-1000

1000-1000

1000-1000

1000-1000

1000-1000

1000-1000

1000-1000

1000-1000

1000-1000

1000-1000

1000-1000

1000-1000

1000-1000

1000-1000

1000-1000

1000-1000

1000-1000

1000-1000

1000-1000

1000-1000

1000-1000

1000-1000

1000-1000

1000-1000

1000-1000

1000-1000

1000-1000

1000-1000

1000-1000

1000-1000

1000-1000

1000-1000

1000-1000

1000-1000

1000-1000

1000-1000

1000-1000

1000-1000

1000-1000

1000-1000

1000-1000

1000-1000

1000-1000

1000-1000

1000-1000

1000-1000

1000-1000

1000-1000

1000-1000

1000-1000

1000-1000

1000-1000

1000-1000

1000-1000

1000-1000

1000-1000

1000-1000

1000-1000

1000-1000

1000-1000

1000-1000

1000-1000

1000-1000

1000-1000

1000-1000

1000-1000

1000-1000

1000-1000

1000-1000

1000-1000

1000-1000

1000-1000

1000-1000

1000-1000

1000-1000

1000-1000

1000-1000

1000-1000

1000-1000

1000-1000

1000-1000

1000-1000

1000-1000

1000-1000

1000-1000

1000-1000

1000-1000

1000-1000

1000-1000

1000-1000

1000-1000

100

2. RESEARCH STATUS

2.1 Laboratory Experiments

2.1.1 Apparatus Development

The observation of the Brownian motion of individual small particles poses several experimental design challenges due to the small scattering cross-section of the submicron particles combined with the short observation time required to resolve the Brownian motion. As a result, the experiment is severely limited by signal to noise considerations, and much effort has focused on refining the optical system to improve the signal to noise ratio.

The optical system which has been assembled for this study is shown schematically in Figure 2.1. A Spectra-Physics Model 165 argon ion laser with a single-line power of approximately 2.5 watts which yields a true TEM₀₀ output with optimum focusing characteristics is used. A Spectra-Physics Model 589 air spaced etalon is inserted into the laser cavity to restrict laser oscillation to a single longitudinal mode. This provides the stable mode amplitude and increased coherence length required in our optical measurement system, but at the expense of a 75% decrease in laser power. The vertically polarized output of the laser is expanded by 25x and collimated to a beam size of approximately 3 cm. The beam expansion leads to tighter focusing and a resultant higher power density at the sample volume than can be achieved with a smaller diameter beam. An adjustable iris diaphragm is used after the beam expander/collimator to select the beam diameter.

The expanded beam is split into two beams (b_R and b_T) by a 50/50 cube beamsplitter, which reflects 50% of the incident light and transmits 35%. An increasing intensity difference in two beams when focused to a point to form interference fringes results in a decreasing clarity of the fringe pattern, which is detrimental to the signal to noise ratio in our optical system.

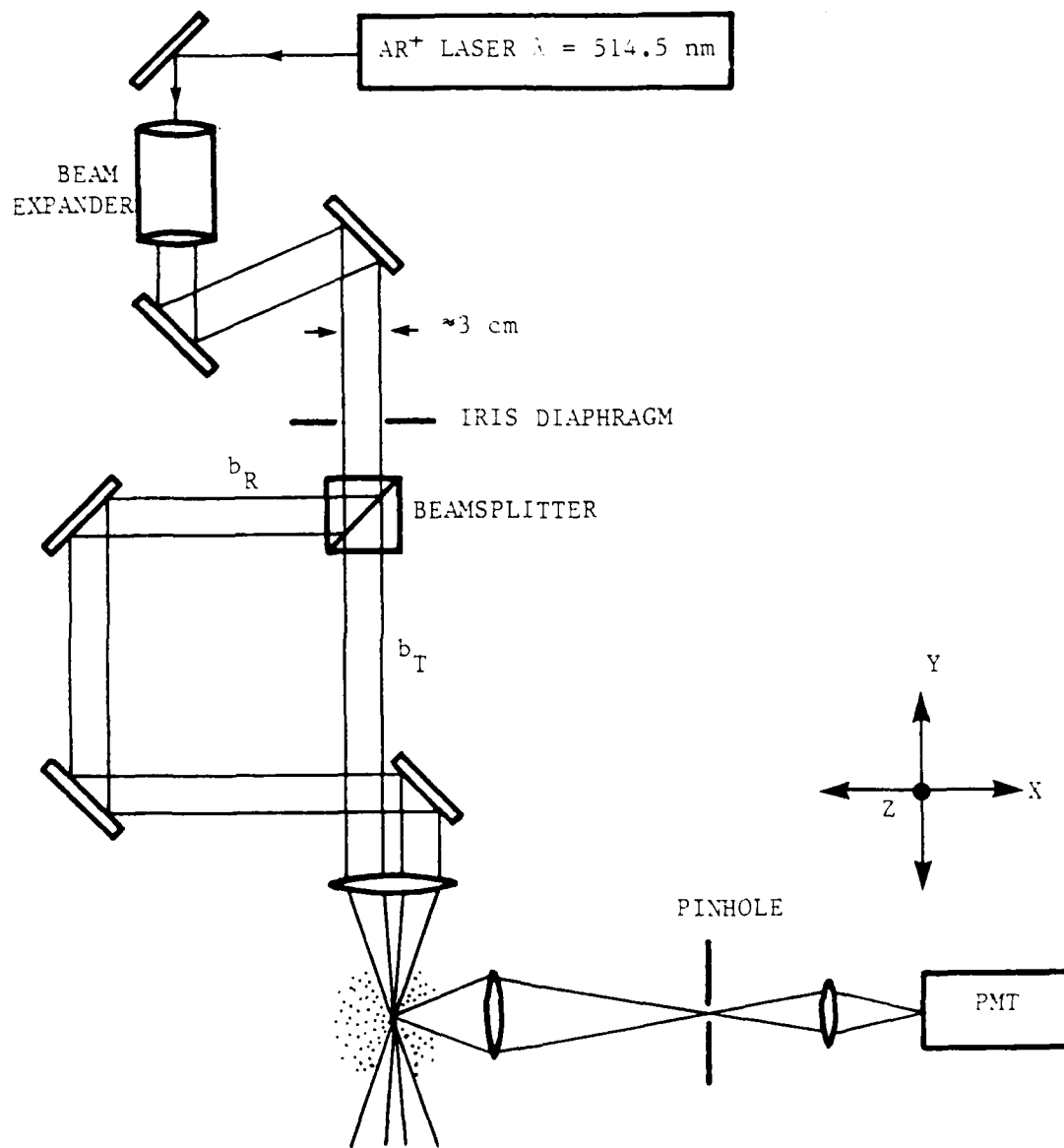


Figure 2.1 Schematic of Experimental Optical System for the Study of Brownian Motion of Individual Submicron Particles.

Therefore, three reflectors are used to decrease the intensity of the reflected beam ($\approx 10\%$ light loss off of each mirror) as well as to position this beam on a path parallel to the transmitted beam (b_T). The two beams of approximately equal intensity are then focused by a multi-element lens to form an interference fringe pattern at the sample volume. The sample volume is imaged through a pinhole and then refocused onto a fast photomultiplier (Type R663) which views the light scattered at 90° . An interference filter is used before the photomultiplier to reject light outside a 1 nm band centered at 514.5 nm.

The measurement volume is defined by the intersection of the laser beam intensity profile and the field of view provided by the pinhole of the receiving optics. Its geometry is depicted in Figure 2.2. The incident beams are at a 7.5° angle with respect to each other and have a total power of 130 milliwatts with the iris diaphragm fully open. The fringe pattern formed from the two beams is easily viewed by magnifying the measurement volume by a factor of 200 and projecting it onto a screen. The number of observed fringes is consistent with a calculated 4 μm fringe spacing and 12 μm beam diameter.

A successful measurement requires the double coincidence that a single particle traverse the fringe system and be detected within the field of view of the receiving optics. Initially, the measurement volume was imaged onto a 25 μm pinhole with a magnification of unity, but low counting rates were observed with such a small field of view. Also, the detection of scattered light through the small pinhole was highly susceptible to random mechanical vibrations. A 400 μm pinhole was subsequently used and the signal detectability was greatly increased, however, the measurement volume was too large. Extraneous signals from the interaction of a single beam with a particle arose because the field of view of 400 μm was not restricted to the overlap region of the two beams. Also, the larger field of view increases the chance of detecting multiple particle events. Presently, the sample volume is imaged with a magnification of ≈ 10 onto a 400 μm pinhole. This is equivalent to a field of view of 40 μm and renders the signal less susceptible to vibrations.

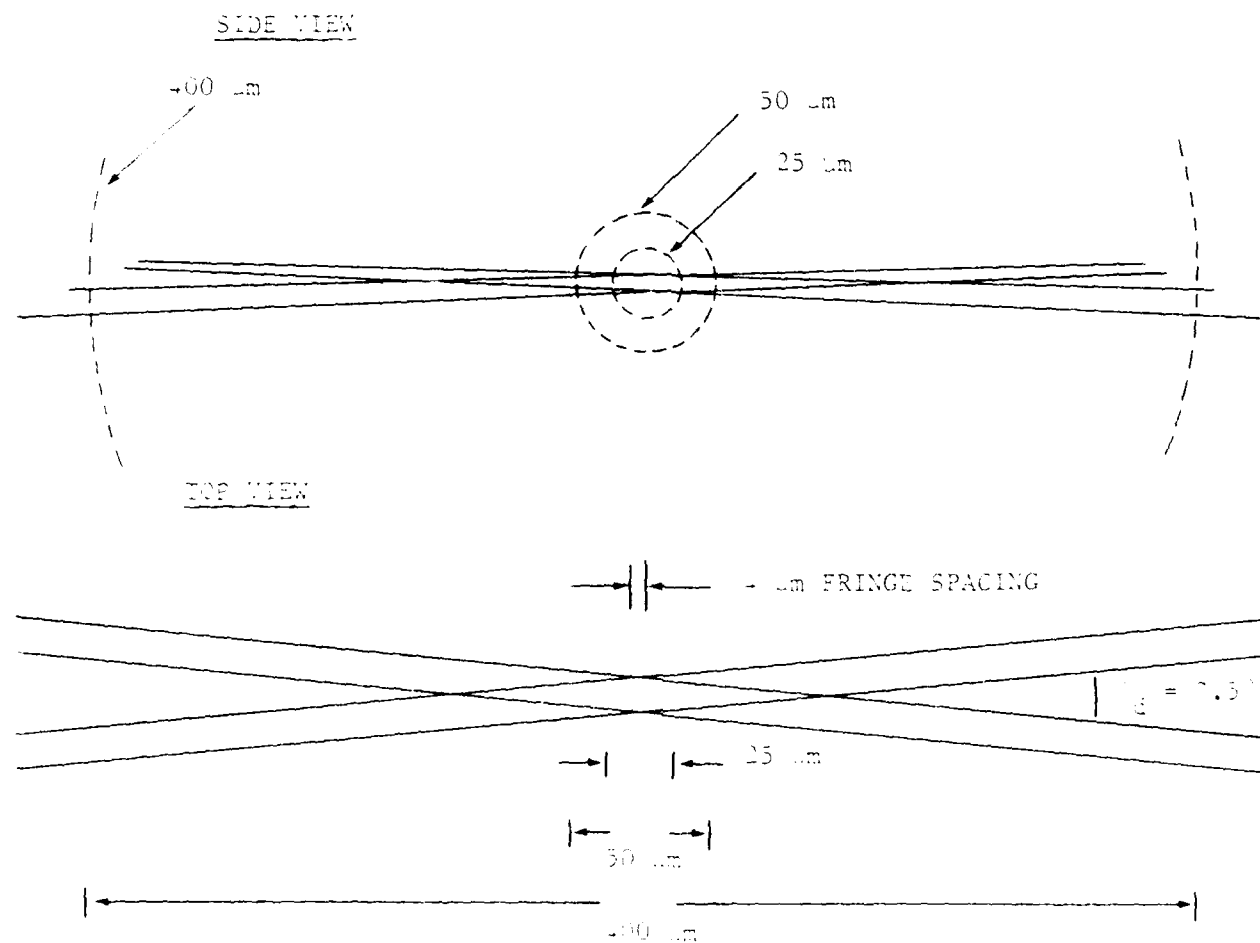


Figure 2.2 Geometry of the Sample Volume, as Seen With the Field of View of 25, 50, and 400 μm Pinholes.

The major experimental obstacle, thus far, has been the proper placement of the pinhole/detector so that the field of view incorporates the limited volume of beam overlap. Several alignment aids have been developed to overcome this difficulty. Spatial overlap of the two beams is verified by magnifying and viewing the image of the focal region, in a manner similar to observing the fringe pattern described earlier. The pinhole, interference filter, lens, and photomultiplier are housed together and are carefully baffled to block out extraneous light. This unit is mounted on an XYZ translation stage to facilitate the critical detector adjustments.

First, the detector must be positioned along the x-axis, i.e., the axis along the scattering direction (See Figure 2.1), so that the image point of the scattered light is at the pinhole. This is best accomplished by inserting a mirror at the focal point of the incident beams and directing the light along the scattered light path. The detector is traversed along its y-axis (perpendicular to the scattered light path) and, at the proper x-axis position the single image of the intense beams viewed after the pinhole appears and disappears. If the pinhole is not at the image point of the beam focus, then traversing the detector along the y-axis leads to a sequential appearance of radiation from each beam while viewing them after the pinhole.

The optimal y and z axis positions of the detector are determined by inserting a 4 μ m diameter wire (TSI Model 1210-T1.5) precisely into the measurement volume focal region as a scattering target. The correct wire position is determined by observing the interference fringes formed by the scattered light and the primary beams. Then, the receiving optics are adjusted for maximum signal.

A microcomputer-based data acquisition system with very fast time resolution capability has been assembled for this project. This system is an IBM Personal Computer XT with a CAMAC interface (DSP Technology, Fremont, Calif.). This system permits considerable flexibility in that any CAMAC-compatible module may be used. Fast time resolution in data acquisition is achieved with the appropriate choice of CAMAC hardware in combination with

fast memories for temporary data storage. The contents of the data memories are transferred into the computer memory via a DMA interface at data rates of approximately 400 kHz. Large volumes of data may then be stored on the system's fixed disk.

Presently, we have set up and tested this system with a fast amplifier/trigger generator (LeCroy Model 0102) and transient recorder (Transiac Model 2001 S) enabling acquisition of up to 32,000 (8-bit) data points at a maximum rate of 100 MHz (10 ns sampling interval).

2.1.2 Particle Measurements

A necessary step in the development of our interferometric optical system to measure individual submicron particles in a gas stream is to verify a standard laser velocimeter mode of operation. Various sources of particles are used to aid in verifying the "LDV" nature of the signal. Representative oscilloscope traces of the scattered light signal are displayed in Figure 2.3. The source of particles in these traces is a stream of H_2O droplets directed through the sample volume.

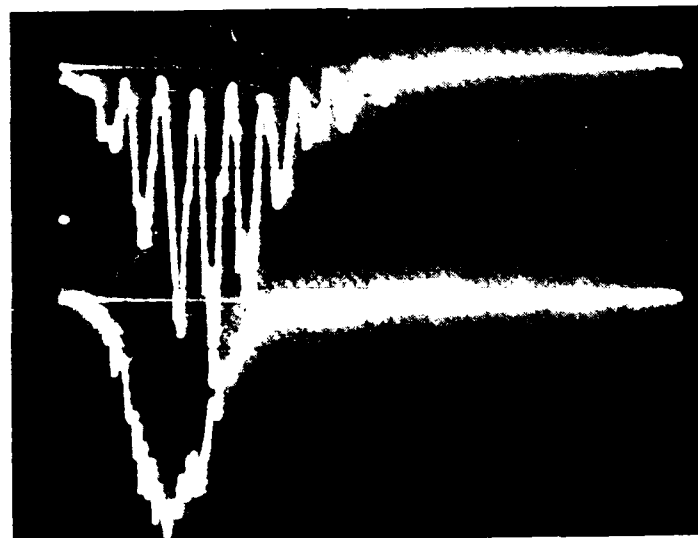
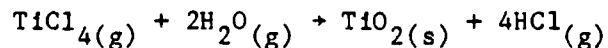


Figure 2.3 Top: Representative Measurement of H_2O Particle Traversing the Sample Volume (x-axis = 1 μs /division).
Bottom: Single-Beam Measurement Taken Under the Same Conditions as Above.

The upper trace illustrates a successful measurement of an individual particle traversing the interference fringe pattern formed from the two incident beams. The signal is nearly 100% modulated which verifies that the beams are of approximately equal intensity and indicates that the diameter of the measured particle is less than or on the order of the calculated 4 μm fringe spacing. The beams, which are only 25% of their 30 mm expanded diameter, are focused to a calculated beam waist of 22 μm based on the observed number of fringes in the trace and the calculated fringe spacing. This is less than a factor of two larger than expected from diffraction limited focusing estimates and confirms that the optics are of sufficient quality to generate the necessary high power densities at the sample volume.

The lower trace in Figure 2.3 is taken with one beam blocked and, therefore, represents an individual particle crossing a single-beam profile, and not an interference fringe pattern. The noise level in the single-beam case is greater than can be accounted for solely by photomultiplier shot noise. Instead, it is probably due to laser noise itself, or some laser interaction along the optical path. Further characterization and subsequent suppression of this noise is being investigated.

Further verification of the "LDV" signal has been achieved by varying the velocity of the droplet stream and observing the expected change in time between fringe crossings by the particle ($\Delta t = \lambda/2nV\sin \theta/2$, where V is the velocity component in the 90° scattering direction). Also, successful measurements have been recorded for individual particles of TiO_2 in a gas stream formed from the chemical reaction:



Although the size distribution of the TiO_2 particles generated by this reaction has not been well characterized, similar formation experiments have yielded TiO_2 size distributions between 0.5 and 0.05 μm in diameter. Future plans include direct characterization of the TiO_2 particles formed in the

laboratory and preparation of other sources of submicron particles in a gas stream.

A complementary and perhaps more exact means of calibrating and characterizing the optical system involves the measurement of particles suspended in liquid solutions. To this end, a particle flow cell has been designed and built in the laboratory which enables us to measure the "LDV" signal from particles of known diameter with the added advantage of well characterized flow velocities. These calibration particles are commercially available (Coulter Electronics) in a variety of sizes in the submicron range. Preliminary measurements of $0.261 \mu\text{m}$ diameter latex particles have been recorded, however, the added alignment difficulties associated with the flow cell requires further refinement of the alignment procedures. These refinements are currently in progress.

2.2 Behavior of the Brownian Motion Signal

2.2.1 Introduction

In the last report,¹ a Monte Carlo simulation of the signal from the Brownian motion sensor was carried out. The result of interest, namely, the time between zero crossings of the Brownian velocity, was found to be dependent on the step size Δt of the simulation. This dependence is actually not surprising because Δt represents essentially the bandwidth of the actual signal detection system, which, being a practical device, should have a finite bandwidth. Since the Brownian motion is a statistical process, the behavior of any signal derived from the Brownian motion is statistical, and the spectral properties of the signal would depend on the bandwidth of the signal detection system. These ideas are further explored here.

In the following, the characteristics of a Brownian motion detection system are first described; the most important result being that the only meaningful information carried by the signal is contained in the time between the extrema, τ , of the signal. Then the theory on the statistical distribution of the values of τ is presented.

2.2.2 The Brownian Motion Detection System

The configuration of a Laser Doppler Brownian motion detection system has been discussed in Reference 1 and elsewhere in this report. For a perfect detection system as a whole, the transfer function is shown in Figure 2.4. By transfer function, we mean the relationship between the input quantity of interest, namely the position of the particle in Brownian motion, and the output signal which is the beat amplitude of the two fringe forming laser beams as seen by a square-law detector.

$$\text{signal} \sim \langle \left| \text{Re}(\underline{E}_1 e^{i\underline{k}_1 \cdot \underline{r}} + \underline{E}_2 e^{i\underline{k}_2 \cdot \underline{r}}) \right| \rangle \quad (1)$$
$$\sim 1 + \cos(\Delta \underline{k} \cdot \underline{r})$$

In the normal LDV application, the particle traverses the illuminated volume with a constant velocity (from A to B in Figure 2.4). If u is the velocity component in the direction of $\underline{k}_1 - \underline{k}_2$,

$$\hat{\Delta \underline{k} \cdot \underline{r}} = u t, \quad (2)$$

the signal will be modulated fully (A'B') as

$$\text{signal} \sim 1 + \cos(\Delta k u t) \quad (3)$$

and the velocity may be obtained from the period τ of the modulation,

$$u = 2\pi/\Delta k \tau \quad (4)$$

Note that implicit in this velocity measurement is a length scale $(\Delta k)^{-1}$ so that a time measurement (τ) can yield a velocity.

In the detection of Brownian motion, however, u is a statistical quantity which changes rapidly in time. In particular, the particle may change

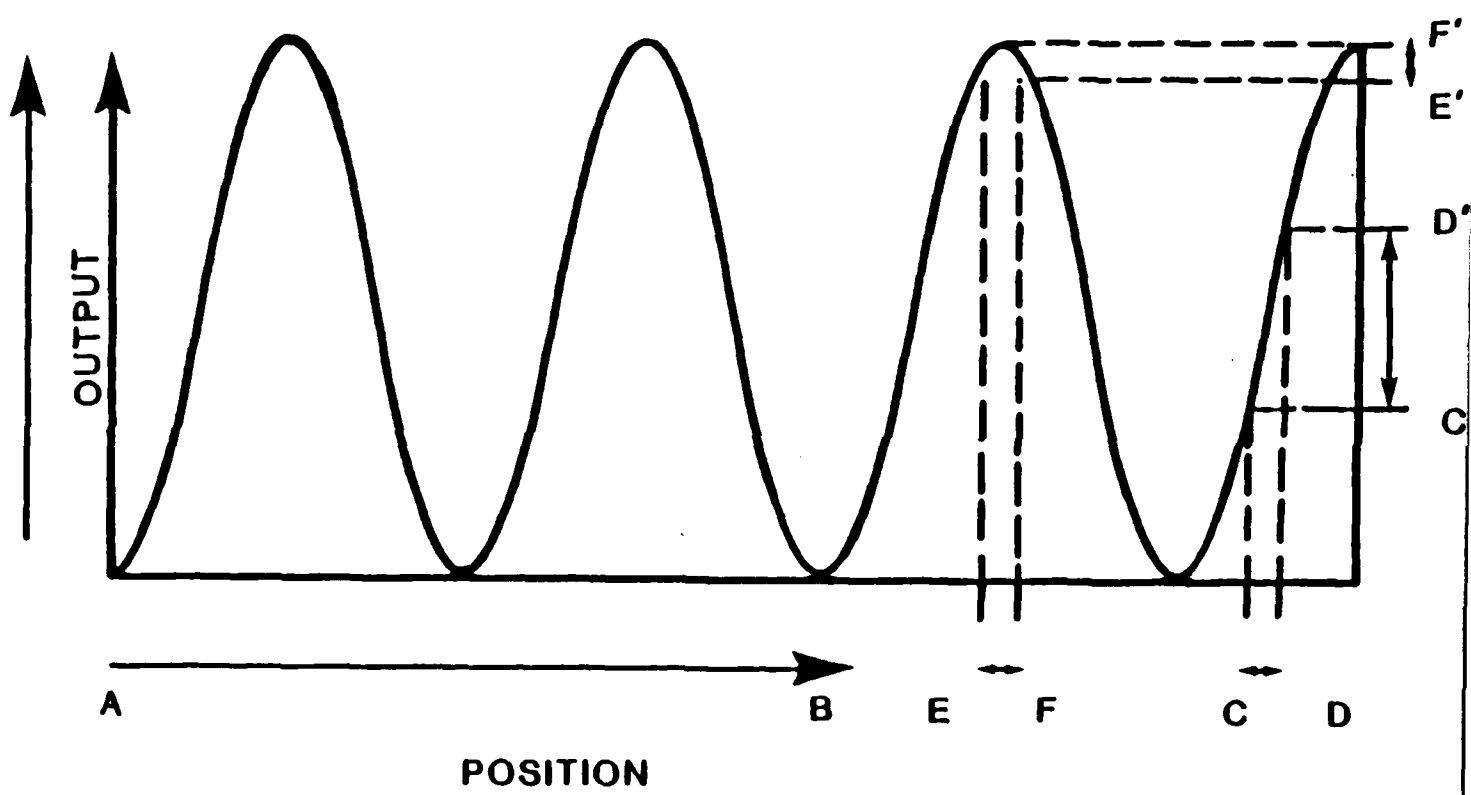


Figure 2.4 Transfer Function of Laser Doppler Velocimeter System.

velocity appreciably (or may even reverse its direction) before it traverses a "fringe" of the transfer function. Therefore the signal is no longer fully modulated and $(\Delta k)^{-1}$ ceases to be a relevant length scale. Because of the nonlinear nature of the transfer function, the amplitude of the signal will not carry meaningful information, e.g., when the particle oscillates about CD in Figure 2.4, the signal response C'D' is quite different from that (E'F') of a similar oscillation EF.

The only meaningful information contained in the signal is the time between the extrema of the signal modulation. Each extremum of the signal represents a reversal in direction of the particle, and therefore, a zero of the Brownian velocity u . In order to interpret the signal, it is necessary to examine the statistical distribution of the zeros of u .

2.2.3 The Statistical Nature of the Brownian Velocity

The Brownian velocity of a particle in thermal equilibrium in a background fluid is described by the Langevin equation. For the observed velocity component u (in the direction of Δk), the Langevin equation is

$$\frac{du}{dt} + \beta u = f \quad (5)$$

where β^{-1} is a relaxation time governed by the mass m and the mobility ϵ of the particle in the fluid.

$$\beta = \frac{1}{\tau_{\text{relax}}} = \frac{\epsilon}{m} \quad (6)$$

The statistical nature of u is due to the random driving force f , which is the result of the impulse arising from each collision of the particle and a molecule of the background fluid. Because these collisions occur randomly, f

may be considered to be a white noise function with a constant spectral density S_f ,

$$\langle f(t)f(t+\tau) \rangle = S_f \delta(t) \quad (7)$$

The time scale associated with the fluctuation of f is of the order of the time between the molecular collisions τ_c , which, for a 100 Å particle in a gas medium at STP is approximately 10^{-11} s. The time response of practical instruments used to observe the Brownian motion velocity is usually much slower than this collision time. The observations, are, therefore, the result of averaging u over a response time scale Δt associated with the instrument, with $\Delta t \gg \tau_c$. The observed value of u is then a random variable, and, since it is the aggregate of many similar events, it would have a Gaussian distribution by the central limit theorem. If the particle has a velocity u_0 at one instant of time, the conditional probability distribution of u at a time Δt later, (so that the value of u is the aggregate of the sum of all the collisions in Δt), is given by.²

$$p(u, u_0; \Delta t) = \frac{1}{\sigma\sqrt{\pi}} \exp \left[-\frac{(u-u_0)^2}{\sigma^2} \right] \quad (8)$$

$$\sigma = \frac{m}{2kT(1-h^2)} \quad (9)$$

Note that the distribution is parameterized by the "memory" factor h

$$h = e^{-\beta \Delta t} \quad (10)$$

and the width σ . The observed velocity $u(t)$ may be viewed as observations at discrete points in time, $t_n = n\Delta t$. When the time step Δt is large compared to the relaxation time ($\beta\Delta t \gg 1$), the velocities u_i are independent of each other, and each obeys a Maxwellian distribution at temperature T . In the

Brownian motion sensor described here, since the velocity amplitude is not measured, all the information is contained in the measurement of the value of β . Therefore, the instrument response time Δt should be such that $\beta \Delta t < 1$. After β is determined, the particle physical properties (ϵ, m) may be determined from Eq. (6).

The Distribution of the Zeros of the Velocity

The Brownian motion sensor measures the time between successive zeros of the Brownian velocity u (in the direction of Δk). The time history of the velocity values, $u(t)$, as observed by an instrument with an integration time Δt , may be thought of as a time series u_n at time $n\Delta t$. From Eq. (8) the values of each u_n are governed by the probability distribution

$$p(u_n, u_{n-1}, \Delta t) = \frac{1}{\sigma\sqrt{\pi}} \exp \left[- \frac{(u_n - u_{n-1}h)^2}{\sigma^2} \right] \quad (11)$$

where the u_{n-1} appears as a parameter. We want to determine the probability $P(N)$ of obtaining a time between two successive zeros of $N\Delta t$.

The problem of determining the distribution of zeros of a random variable has been studied extensively in the context of shot noise in electronic devices, and in queueing theory. The classic review of the subject is given in Reference 3. We shall derive the expression for $P(N)$ independently here. To connect our result to that in the literature of noise current, the random driving force f in Eq. (5) may be considered as the randomly arriving electron, and the observed "current" u is the result of two transfer functions (or filters) in series. The first transfer function is that associated with the Langevin equation. Formally

$$u(t) = \int_{-\infty}^{\infty} \hat{f} e^{-i\omega t} \frac{e^{-(\beta t i\omega)}}{(2\pi)} \frac{d\omega}{2\pi} \quad (12)$$

where \hat{f} is the Fourier Transform of f . Physically, this transfer function is due to the averaging of the effect of f by the damping of the particle in the fluid. The second transfer function is due to the averaging by the instrument. Therefore the overall transfer function is

$$u(t) = \frac{1}{\Delta t} \int_{t-\Delta t}^t dt' \int_{-\infty}^{\infty} \frac{\hat{f} e^{i\omega t'}}{(\beta t i \omega)} \frac{d\omega}{2\pi} \quad (13)$$

It should be noted that no closed form solutions for $P(N)$ have been worked out, except for rather trivial cases. The difficulty was attributed³ to the lack of an analytical solution to the N dimensional integral involved.

We shall derive the expression for $P(N)$ here. The process of obtaining a successive zero in N steps may be described as the following. At time zero ($n = 0$), the particle has a very small velocity δu , which, within the amplitude resolution of the instrument, may be considered as zero. In the following argument, δu is taken as positive. The argument will be exactly the same if δu is negative. We shall define a zero-crossing event at $t = N\Delta t$, ($n = N$), as an event with velocity greater than zero at $t = (N - 1)\Delta t$, ($n = N - 1$), and velocity less than or equal to zero at $t = N\Delta t$. The time resolution of this definition of zero-crossing is Δt , and so the meaning of such an event for $N = 1$ is not precise. Then the condition for occurrence of a successive zero in N time steps is to have the velocities be positive for $n = 1, \dots, N-1$; and the velocity be negative or equal to zero for $n=N$.

Therefore

$$P(N) = \int_0^{\infty} du_1 p(u_1, 0; \Delta t) \int_0^{\infty} du_2 p(u_2, u_1; \Delta t) \dots \quad (14)$$

$$\dots \int_0^{\infty} du_{N-1} p(u_{N-1}, u_{N-2}; \Delta t) \int_{-\infty}^0 du_N p(u_N, u_{N-1}; \Delta t)$$

Using the formula for p in Eq. (11), and changing the variable from u to $\xi = u/\sigma$, the above probability becomes

$$P(N) = \left(\frac{1}{\sqrt{\pi}}\right)^N \int_0^\infty d\xi_1 e^{-\xi_1^2} \int_0^\infty d\xi_2 e^{-(\xi_2 - \xi_1 h)^2} \dots \dots \int_0^\infty d\xi_{n-1} e^{-(\xi_{n-1} - \xi_{n-2} h)^2} \int_{-\infty}^\infty d\xi_n e^{-(\xi_n - \xi_{n-1} h)^2} \quad (15)$$

Note that σ does not appear in this expression. This is because the zero-crossing time pertains to the zeros of the velocity, and is therefore independent of the velocity scale. (The value σ is a velocity scale measuring the width of the velocity distribution).

If the integration time Δt is large ($3\Delta t \gg 1$), h will approach zero and Eq. (15) reduces to a binomial process

$$P(N) = \left(\frac{1}{2}\right)^N \quad (16)$$

The average value of N is

$$\bar{N} = \sum_{N=1}^{\infty} N P(N) = \sum_{N=1}^{\infty} \frac{N}{2^N} = \frac{d}{dx} \left| \sum_{x=1}^{\infty} \left(\frac{x}{2}\right)^N \right| = 2 \quad (17)$$

In this case, the data values corresponding to the successive zeroes of the velocity become a completely random sequence, and do not carry information about h .

For small values of h , the multiple integral may be worked out as follows: An operator I_n is defined as

$$I_n(f(\xi_n)) \equiv \frac{1}{\sqrt{\pi}} \int_0^\infty d\xi_n e^{-(\xi_n - \xi_{n-1}h)^2} f(\xi_n) \quad (18)$$

The quantity ξ_{n-1} enters as a parameter in the above definition. Then

$$I_n(1) = \frac{1}{2} (1 + \frac{2}{\sqrt{\pi}} \xi_{n-1} h) + O(h^2) \quad (19)$$

$$I_n(\xi_n h) = \frac{1}{2} \frac{h}{\sqrt{\pi}} + O(h^2) \quad (20)$$

The expression for $P(N)$, Eq. (15), after evaluating the last integral on the right hand side, becomes

$$P(N) = \frac{1}{2} I_1 I_2 \dots I_{N-1} (1 + \frac{2}{\sqrt{\pi}} \xi_{N-1} h) + O(h^2) \quad (21)$$

The expression (19) and (20) may be used repeatedly in (21). The first few expressions are:

$$P(N) = \left(\frac{1}{2}\right)^2 I_1 \dots I_{N-2} \left[(1 - \frac{2h}{\pi}) + \frac{2}{\sqrt{\pi}} \xi_{N-2} h \right] + O(h^2)$$

$$= \left(\frac{1}{2}\right)^3 I_1 \dots I_{N-3} \left[1 + \frac{2}{\sqrt{\pi}} \xi_{N-3} h \right] + O(h^2)$$

$$= \left(\frac{1}{2}\right)^4 I_1 \dots I_{N-4} \left[(1 + \frac{2h}{\pi}) + \frac{2}{\sqrt{\pi}} \xi_{N-4} h \right] + O(h^2)$$

•
•
•

$$P(N) = \left(\frac{1}{2}\right)^N \left[1 + (N-3) \frac{2h}{\pi}\right] + O(h^2); N \geq 2 \quad (22)$$

The above expression is valid for $N \geq 2$. For $N = 1$, since the velocity at $n = 0$ is preconditioned to be ≈ 0 ,

$$P(1) = \int_{-\infty}^0 e^{-(\xi_1 - 0)^2} d\xi_1 = \frac{1}{2} \quad (23)$$

Compared to the binomial distribution ($P(N) = 2^{-N}$), which is the limit for $h = 0$, $P(N)$ decreases with h for $N < 3$ and increases with h for $N > 3$. This result is illustrated in Figure 2.5. Since the velocity at $n = 0$ is zero, the velocity u_1 at $n = 1$ is sampled from a Gaussian centered at zero. The value of $P(N = 1)$ is the probability that this velocity is negative, and $P(1)$ is therefore $1/2$. Say the velocity at $n = 1$ is $u_1(> 0)$, then the velocity u_2 at $n = 2$ is sampled from a Gaussian centered at $u_1 h$. The probability of u_2 being negative is the shaded area in Figure 2 under the Gaussian at $n = 2$, and this value is $< 1/2$ for $h > 0$. Therefore $P(2) < (1/2)^2$. For $N = 3$, the probability of obtaining a consecutive zero here is represented by the shaded area under the Gaussian centered at $u_2 h$ at $n = 3$ (Figure 2.5). This area has to be summed over all the realizations of the possible values of positive u_2 , which is sampled from the Gaussian centered at $u_1 h$, which again has to be summed over all the realizations of u_1 . Although the shaded area at $n = 3$ is less than $1/2$, there are "more" realizations than the $h = 0$ case because u_2 is sampled from the shifted Gaussian. These two effects balance each other to $O(h^2)$, and $P(3)$ is equal to $(1/2)^3 + O(h^2)$. For $N > 3$, $P(N)$ is given by Eq. (22), and is greater than $(1/2)^N$. The values of $P(N)$ are plotted versus N in Figures 2.6 and 2.7.

It is not possible to obtain a closed form solution of $P(N)$ for arbitrary h ($h < 0 < 1$ corresponding to $0 < \beta \Delta t < \infty$) because of the difficulty in evaluating the multiple integral in Eq. (11). Direct numerical calculation of

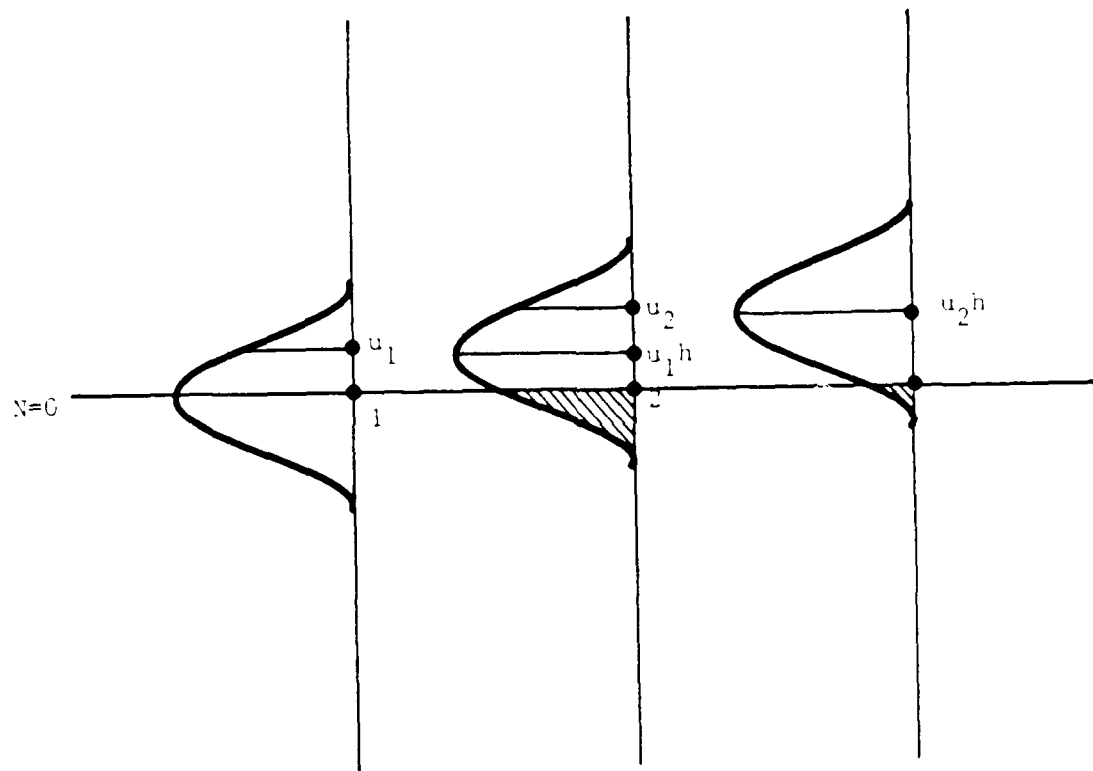


Figure 2.5 Velocity Sampling at the First 3 Time Steps.

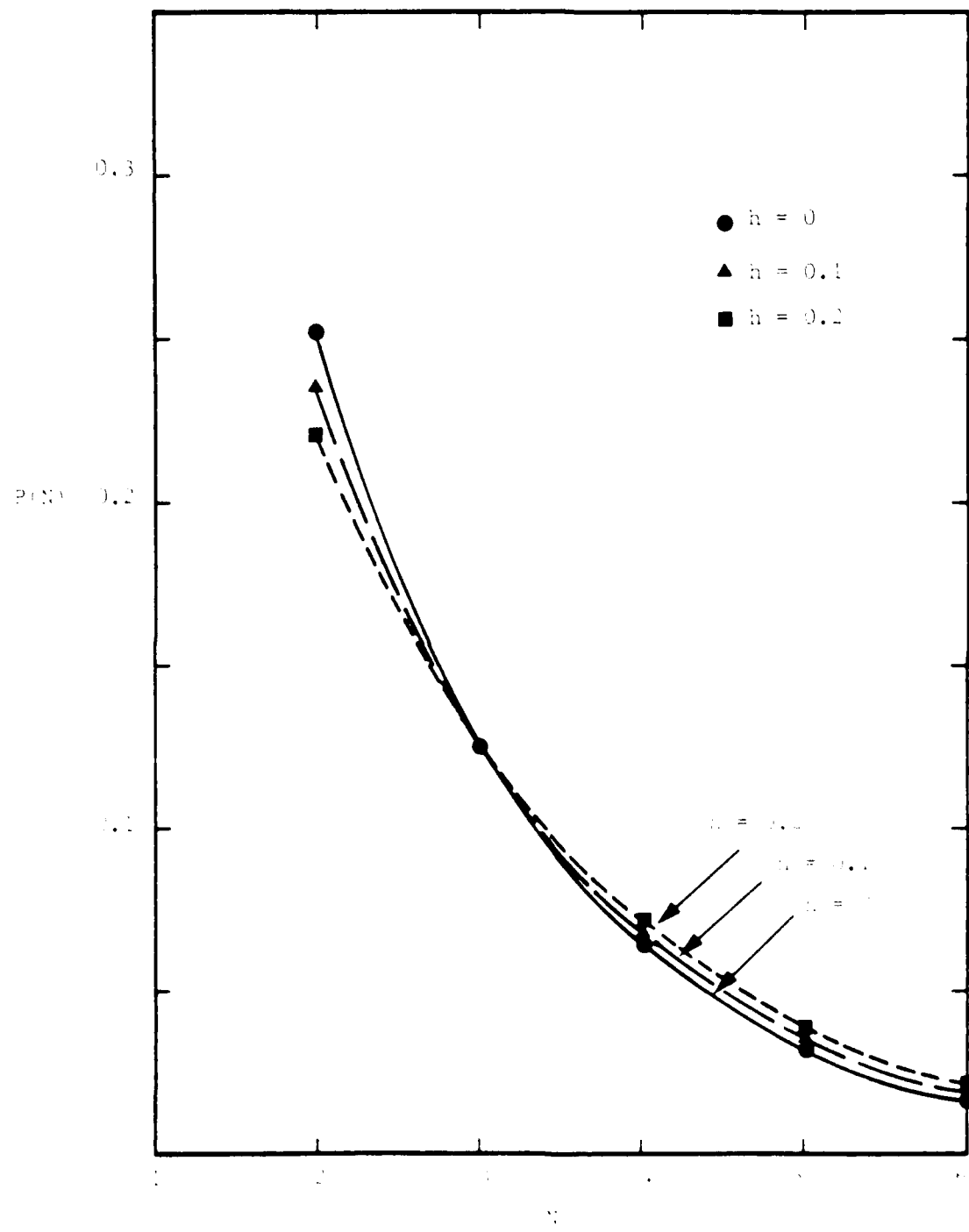


Figure 2.6 Probability of Obtaining a Consecutive Zero of the Brownian Velocity in N Steps (Linear Scale).

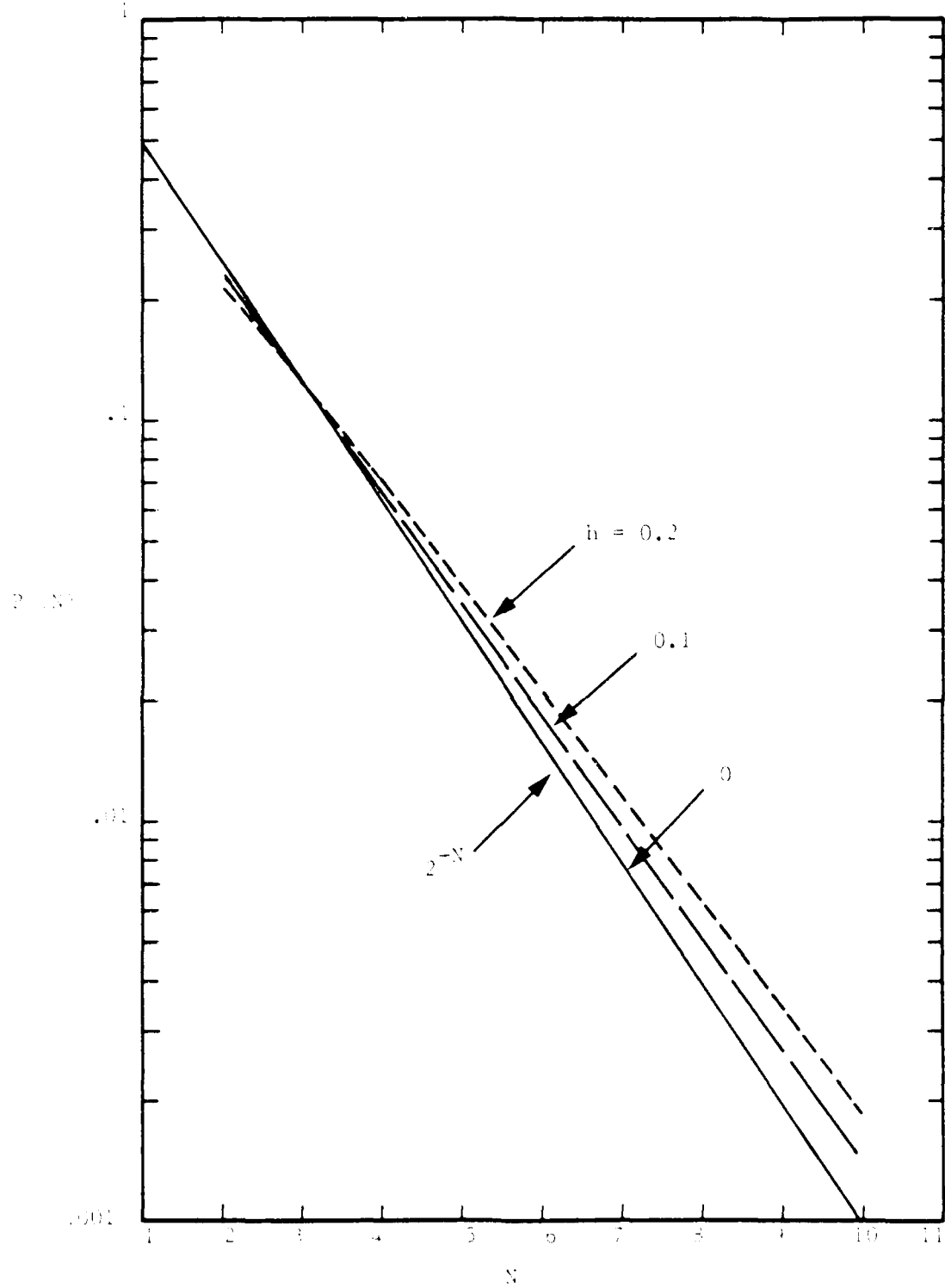


Figure 2.7 Probability of Obtaining a Consecutive Zero of the Brownian Velocity in N Steps (Semi-Log Scale).

the integral is not feasible for any large N , say $N > 5$. Monte Carlo evaluation of the integral would be equivalent to our earlier simulation of the Brownian motion.¹ The results from Reference 1 will be reexamined in this context here.

The general behavior of the mean number of steps \bar{N} between consecutive zero-crossings of the Brownian velocity is shown in Figure 2.8. For $h = 0$, \bar{N} is 2 (from Eq. (17)). For small h ,

$$\begin{aligned}\bar{N} &= \sum_{N=1}^{\infty} N \left(\frac{1}{2}\right)^N \left(1 + (N-3) \frac{2h}{\pi}\right) + O(h^2) \\ &= \sum_{N=1}^{\infty} \left(\frac{N}{2^N}\right) \left(1 - \frac{6h}{\pi}\right) + \sum_{N=1}^{\infty} \left(\frac{N^2}{2^N}\right) \left(\frac{2h}{\pi}\right) + O(h^2) \\ \bar{N} &= O(h^2) \end{aligned} \quad (24)$$

In the last expression, we made use of $\sum(N/2^N) = 2$ and $\sum(N^2/2^N) = 6$. Therefore $\bar{N} = O(h^2)$ for small h . For large relaxation time ($\beta \rightarrow 0$, $\beta\Delta t \rightarrow 0$, and $h \rightarrow 1$), the particle, once it acquires a positive (or negative) velocity, will retain that velocity for a large time. Consequently $\bar{N} \rightarrow \infty$.

The results of the Monte Carlo simulation in Reference 1 have been replotted in the context of the present analysis in Figure 2.9, and confirm the theory. The results in Figures 2.8 and 2.9 show that to obtain h , (and therefore the values of β , which would lead to the values for ξ/m), it is necessary to have a time resolution of Δt such that $\beta\Delta t \ll 1$ (or $h = e^{-\beta\Delta t}$ close to 1).

2.2.4 Conclusion

A theoretical analysis of the probability of obtaining a time τ between consecutive zero-crossings of the Brownian velocity u has been presented.

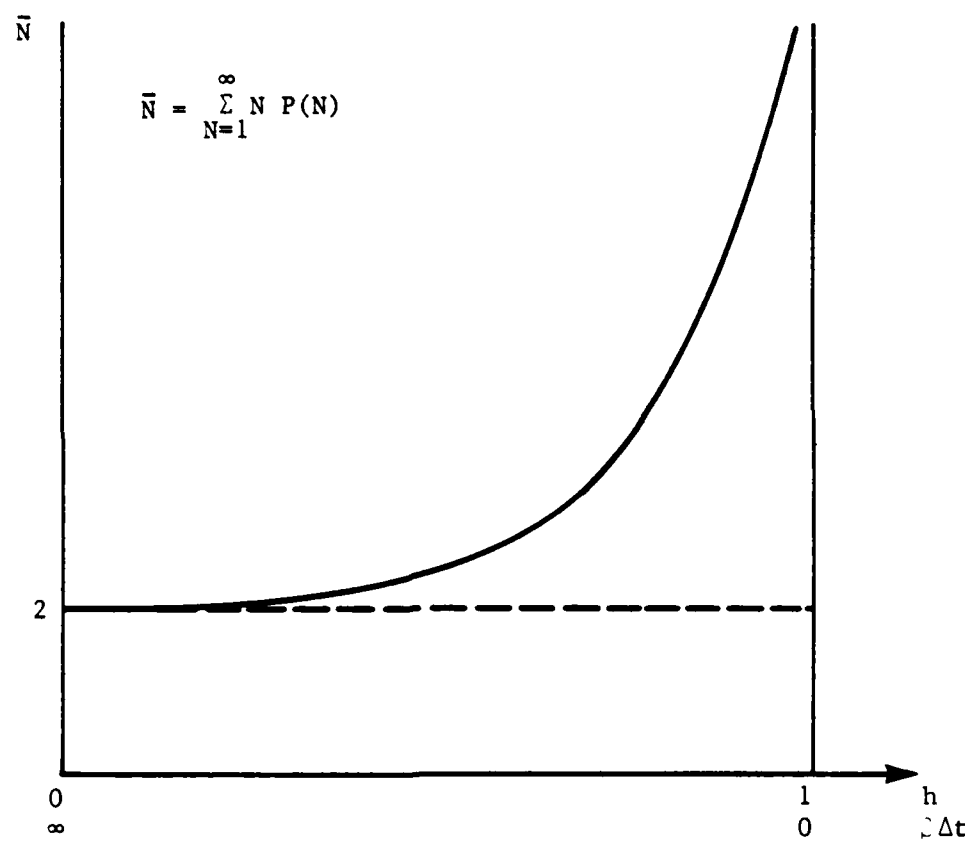


Figure 2.8 General Behavior of the Expectation Value of the Number of Time Steps Between Consecutive Zero-Crossings of the Brownian Velocity, as a Function of the Memory Parameter $h = \exp(-\beta \Delta t)$.

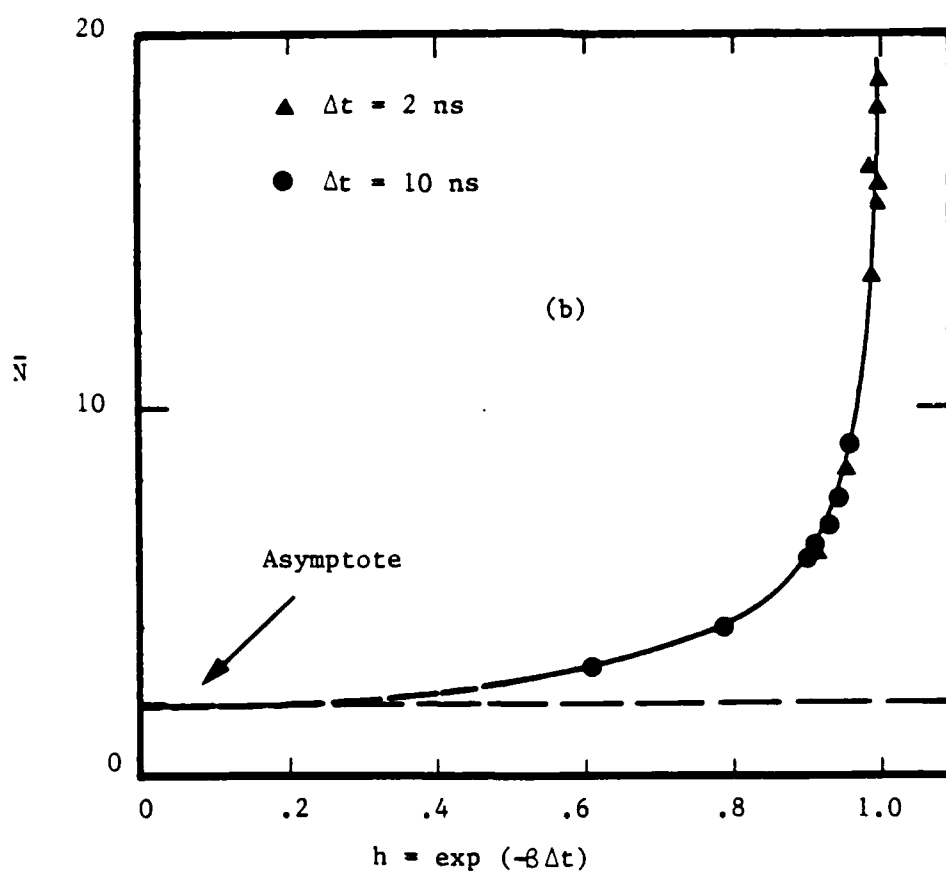
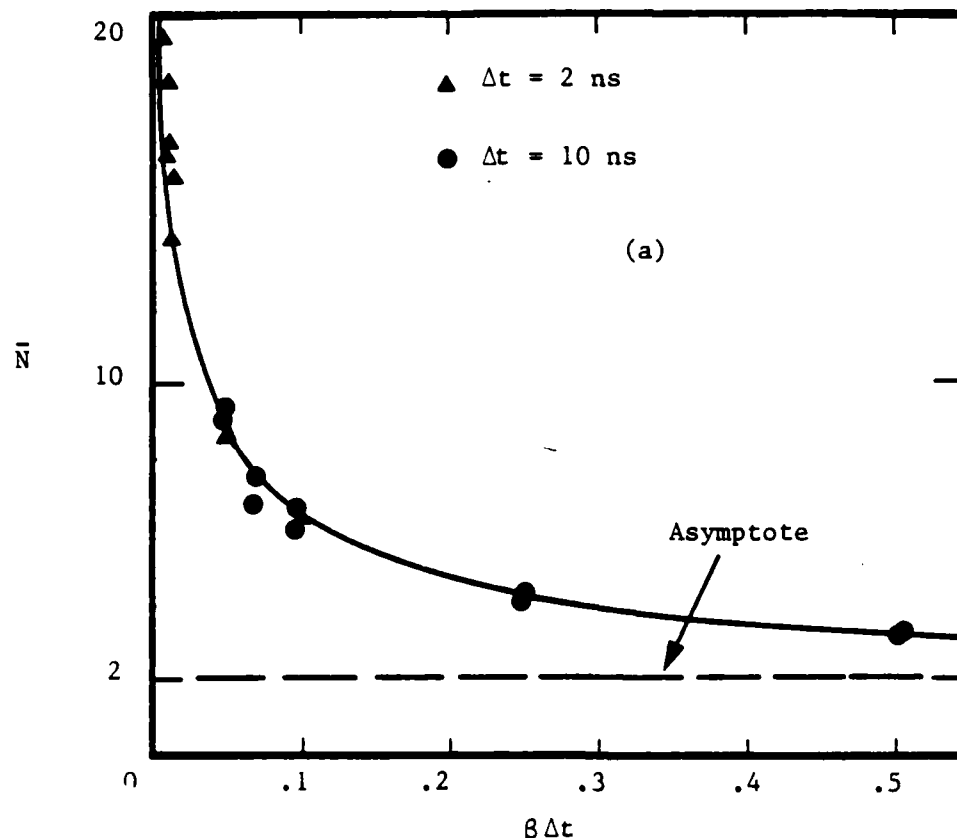


Figure 2.9 Monte Carlo Simulation Result of the Mean Time Step (\bar{N}) Between Zero-Crossings of the Velocity, (a) as a Function of $\beta \Delta t$; (b) as a Function of $h = e^{-\beta \Delta t}$.

Since u is a random variable, the probability $P(\tau)$ is necessarily a function of the integration time Δt of the instrument used to observe u . The analysis has been carried out in terms of discretizing the time in steps of Δt , $t_n = n\Delta t$, and the resulting probability $P(N)$, ($N = \tau/\Delta t$), has been derived. The values of $P(N)$ are found to be dependent on the "memory" h ($h \equiv \exp(-\beta\Delta t)$) of the Brownian velocity, where β^{-1} is the relaxation time. For very short memory ($h \ll 1$), the probability $P(N)$ tends to the binomial limit $P(N) = 1/2^N$. The expectation value \bar{N} ($\equiv \sum N P(N)$) assumes the value of 2 in the binomial limit and $2 + O(h^2)$ for small h . For large relaxation time ($\beta \rightarrow 0$), $\bar{N} \rightarrow \infty$. To obtain accurate information from the measurement of \bar{N} about h , and therefore, the value of β which is related to the physical properties of the particle suspended in the fluid, it is necessary to have $\beta\Delta t < 1$. Since the result is a function of the integration time Δt , which is not a precisely defined quantity for the measuring instrument, the Brownian motion sensor must be a calibrated instrument.

2.3 Research Plan

The research plan for the third year of the program will continue to emphasize experimental validation of the measurement concept. Specifically, we anticipate performing the following tasks:

Task 1.

We will continue the measurements of particles of known size suspended in liquids in order to maximize the signal to noise of our optical measuring system, to refine our data acquisition methods, and to verify our theoretical understanding of the acquired signal. Data from these commercially available particles in the $0.046 \mu\text{m}$ to $0.5 \mu\text{m}$ size range should help establish the limitations of our apparatus. Analysis of the signal from the different size particles, when compared to the Monte Carlo simulations, should establish whether the signal fluctuations exhibit the expected behavior for particles of different size, and should provide a crucial test for the measurement theory.

Task 2.

If the tests with liquid suspensions conclude with favorable results, we will proceed with measurements of submicron particles suspended in gas flows. These measurements will proceed in two steps:

- a. The well defined liquid-suspended particles described in Task 1 will be dispersed into a gas stream. The results from such monodisperse particulates will be compared to the measurements obtained in liquid suspensions.
- b. We are currently researching methods of chemical generation of small particulates from the gas phase. Likely methods include the TiO₂ generation described in this report and photochemical particulation induced by a pulsed N₂ laser in a CS₂ vapor. The size distribution results obtained from these gas-borne particulates in our Laser Doppler measurement system will be compared to distributions obtained via an independent method such as electron microscopy. The measurements of submicron particles suspended in well controlled gas flows should be critical in establishing the capabilities and limitations of the technique as a particle diagnostic.

References

1. Stanton, A.C. and Cheng, W.K., "Study of Submicron Particle Size Distribution by Laser Doppler Measurement of Brownian Motion," ARI-RR-423, Annual Technical Report, October 1984.
2. Chandrascklar, S., "Stochastic Problems in Physics and Astronomy," *Reviews of Modern Physics*, Vol. 15, 1, 1943.
3. Rice, S.O., "Mathematical Analysis of Random Noise," *Bell System Technical Journal*, Vol. 23 and 24.

3. PUBLICATIONS

No results to date from this program have been published in technical journals. We anticipate two publications in the coming year, one reporting the theory and experimental validation of the Brownian motion measurement approach (to be submitted to Journal of Applied Physics or Physics of Fluids) and a second paper describing a measurement application (to be submitted to Applied Optics).

4. PERSONNEL

The Principal Investigators for this work are Dr. Alan Stanton, who is a Principal Research Scientist at Aerodyne Research, Inc., and Dr. Wai Cheng, Principal Research Scientist (part-time) at Aerodyne and Associate Professor of Mechanical Engineering, MIT. Dr. Stanton has concentrated his research efforts to date for this program on the development of optical and data acquisition systems for the experimental program, while Dr. Cheng has concentrated on the measurement theory, through development of the Monte Carlo Brownian motion simulation model. In addition to his work at Aerodyne on this project, Dr. Cheng has supervised the work of undergraduate and graduate students in the Department of Mechanical Engineering, MIT. This work has been in support of the Brownian motion simulation model, funded by a subcontract to MIT.

The laboratory implementation of this program has been mostly performed by Mr. Keith McCurdy, who joined the staff of Aerodyne this past year as a Research Scientist. Mr. McCurdy recently received his Master's degree in physical chemistry from Rice University.

5. INTERACTIONS

One invited presentation on this work was made during the past year:

W.K. Cheng, A.C. Stanton, and K. McCurdy, "Single Particle Sizing by Measurement of Brownian Motion," Particulate Emission Technology Meeting, Monterey, CA, April 16-18, 1985.

6. NEW DISCOVERIES OR INVENTIONS

The experimental approach under study in this program, i.e., determination of particle size by measurement of the Brownian motion of individual particles, is a new approach which has not previously been demonstrated. We anticipate that this approach, if successful, will permit the development of research instrumentation for the study of the growth of submicron particles, based on new concepts in measurement and data analysis.

E

W

D

II - 8

DTIC